

# Blackfolds

Roberto Emparan

*Institució Catalana de Recerca i Estudis Avançats (ICREA)*

*and*

*Departament de Física Fonamental and Institut de Ciències del Cosmos,  
Universitat de Barcelona, Martí i Franquès 1, Barcelona, Spain*

## Abstract

This is an introduction to the blackfold effective worldvolume theory for the dynamics of black branes, as well as its use as an approximate method for the construction of new black hole solutions. We also explain how the theory is useful for the analysis of dynamical, non-stationary situations, in particular of the Gregory-Laflamme instability of black branes.

## 1 Introduction

The existence of black  $p$ -branes in higher-dimensional General Relativity hints at the possibility of large classes of black holes without any four-dimensional counterpart. Black rings provide a nice explicit example: in [1] they were introduced as the result of bending a black string into the shape of a circle and spinning it up to balance forces. One can naturally expect that this heuristic construction extends to other black branes. If the worldvolume of a black  $p$ -brane could be similarly bent into the shape of a compact hypersurface, for instance a torus  $\mathbb{T}^p$  or a sphere  $S^p$ , we would obtain many new geometries and topologies of black hole horizons.

Unfortunately, the techniques that allow to construct *exact* black hole solutions in four and five dimensions have not been successfully extended to more dimensions. Still, one may want to hold on to the intuition that a long circular black string, or more generally a smoothly bent black brane, could be obtained as a perturbation of a straight one.

The experience with brane-like objects in other areas of physics suggests that such approximate methods may be efficiently applied to this problem. Consider, for instance, the Abelian Higgs theory and its familiar string-like vortex solutions. These are first obtained in the form of static, straight strings, but one expects that they can also bend and vibrate. It has been long

recognized that, if the wavelength of these deformations is much longer than the thickness of the vortex, the dynamics of the full non-linear theory is well approximated by the simpler Nambu-Goto worldsheet action. One can then use it for studying loops of strings of diverse shape. Another example is provided by D-branes in string theory, which are defined as surfaces where open strings can attach their endpoints. Although the bending and vibrations of D-branes are generally intractable in an exact manner in string theory, they are again very efficiently captured by the Dirac-Born-Infeld worldvolume field theory, which is applicable as long as the scale of the deformations is sufficiently large that locally the brane can still be well approximated as a flat D-brane. In all these cases, the full dynamics of the brane is replaced by an effective worldvolume theory for a set of “collective coordinates”.

So, similarly, we seek an effective theory for describing black branes whose worldvolume is not exactly flat, or not in stationary equilibrium, but where the deviations from the flat stationary black brane occur on scales much longer than the brane thickness. Black branes whose worldvolume is bent into the shape of a submanifold of a background spacetime have been named *blackfolds*.

This chapter introduces the blackfold effective worldvolume theory for the dynamics of black branes, as well as its use as an approximate method for the construction of new black hole solutions [2, 3, 4]. Of special interest is a class of helical black rings that provide the first example of black holes in all  $D \geq 5$  with the minimum of symmetry required by rigidity theorems. We also explain how the theory is useful for the analysis of dynamical, non-stationary situations, in particular of the Gregory-Laflamme instability of black branes reviewed in [5]. The blackfold techniques connect it very directly to the instability of an effective “black brane fluid”, in a manner that shares features with the fluid/gravity correspondence of [6].

A word about notation in this chapter. When considering a  $p$ -brane with worldvolume  $\mathcal{W}_{p+1}$  embedded in a  $D$ -dimensional background spacetime, we denote

$$n = D - p - 3. \tag{1.1}$$

Spacetime indices  $\mu, \nu$  run in  $0, \dots, D$  and the covariant derivative compatible with the background metric  $g_{\mu\nu}(x)$  is  $\nabla_\mu$ . Worldvolume indices  $a, b$  run in  $0, \dots, p$ , and the covariant derivative compatible with the metric  $\gamma_{ab}(\sigma)$  induced on  $\mathcal{W}_{p+1}$  is  $D_a$ .

## 2 Effective theory for black hole motion

Above we have motivated the blackfold effective approach by drawing analogies between black branes and the extended brane-like solutions of other non-linear theories. However, the general-relativistic aspects of the effective theory of black  $p$ -brane dynamics are better introduced by considering first the simpler case of  $p = 0$ : the effective dynamics of a black hole that moves in a background whose curvature radii  $\sim R$  are large compared to the black hole horizon radius  $r_0$ ,

$$r_0 \ll R. \quad (2.1)$$

This separation of scales implies the existence of two distinct regions in the geometry. First, there is a region around the black hole where the geometry is well approximated by the Schwarzschild(-Tangherlini) solution. If in this “near zone” we choose a coordinate  $r$  centered at the black hole, the Schwarzschild geometry is a good approximation as long as  $r \ll R$ , i.e.,

$$ds_{(near)}^2 = ds^2(\text{Schwarzschild}) + O(r/R). \quad (2.2)$$

The corrections to the Schwarzschild metric are the (tidal) distortions that the background curvature creates on the black hole.

The second region is far enough from the black hole that its effect on the background geometry is very mild and can be treated as a small perturbation. This is the “far zone” where  $r \gg r_0$ , and in which we can expand

$$ds_{(far)}^2 = ds^2(\text{background}) + O(r_0/r). \quad (2.3)$$

Since we are too far from the black hole to resolve its size, effectively it is a pointlike source whose gravitational effect on the background can be computed perturbatively. To this source we can assign an effective trajectory  $X^\mu(\tau)$ , with proper time  $\tau$  and with velocity  $\dot{X}^\mu = \partial_\tau X^\mu$  such that  $g_{\mu\nu} \dot{X}^\mu \dot{X}^\nu = -1$ . We also ascribe to it an effective stress-energy tensor that encodes how the black hole affects the gravitational field in the far zone.

Let us determine the general form of this stress-energy tensor. We can naturally assume that the acceleration and other higher derivatives of the particle’s velocity are small, since they must be caused by the deviations away from flatness of the background in the region where the black hole moves. Since these variations occur on scales  $\sim R$ , these higher-derivative terms must be suppressed by powers of  $r_0/R$ . To leading order in this expansion, the stress-energy tensor of the effective source is fixed by symmetry and worldline reparametrization invariance to have the form

$$T^{\mu\nu} = m \dot{X}^\mu \dot{X}^\nu. \quad (2.4)$$

In principle the coefficient  $m$  can also depend on  $\tau$ . This tensor is understood to be localized at  $x^\mu = X^\mu(\tau)$ .

In effect, we are replacing the entire near-zone geometry with a pointlike object. In the language of effective field theories, we are ‘integrating out’ the short-wavelength degrees of freedom of the near-zone, and replacing them with an effective worldline theory of a point particle. The coefficient  $m$  must then be related through a matching calculation to a parameter of the ‘microscopic’ configuration, which in this case can only be the horizon size  $r_0$ . The matching condition is that the gravitational field of the effective source reproduces that of the black hole in the far zone. Thanks to the separation of scales (2.1) the near and far zones overlap in

$$r_0 \ll r \ll R \tag{2.5}$$

so we can match the fields there. In this region, the near-zone Schwarzschild solution is in a weak-field regime and can be linearized around Minkowski spacetime. On the other hand, the background curvature of the far-zone geometry can be neglected in (2.5), so the far field is the linear perturbation of Minkowski spacetime sourced by (2.4). It is now clear that these two fields are the same if  $m$  is equal to the ADM mass of the Schwarzschild solution with horizon radius  $r_0$ , so<sup>1</sup>

$$m = \frac{(D-2)\Omega_{D-2}}{16\pi G} r_0^{D-3}, \tag{2.6}$$

where  $\Omega_{D-2}$  is the volume of the unit  $(D-2)$ -sphere. This result is the first step in the method of “matched asymptotic expansions” [7]. One can now proceed to solve the Einstein equations in a perturbative manner, first in the far-zone, including the backreaction from the particle with suitable asymptotic conditions, and then in near-zone, where horizon regularity is imposed. At each step, the solution in one zone provides boundary conditions for the equations to be solved in the other zone, through the matching of fields in the overlap region. Corrections involve higher derivatives of the velocity and of  $r_0$ .

In this matching construction, a subset of the Einstein equations can be written as equations for  $r_0(\tau)$  and  $X^\mu(\tau)$ . Their derivation is a well-understood but technically complicated procedure. Fortunately, if we are only interested in the leading order equations we can use a shortcut to them by applying a main guiding principle of effective theories: symmetry

<sup>1</sup> Note that  $m = \dot{X}^\mu \dot{X}^\nu T_{\mu\nu} = T_{\tau\tau}$  is proportional, but not necessarily equal, to the mass measured at asymptotic infinity in the background. The relation is given by the redshift between the particle’s proper time and the asymptotic time of the background.

and conservation principles. In this case the principle is general covariance, which imposes that

$$\overline{\nabla}_\mu T^{\mu\nu} = 0. \quad (2.7)$$

This is indeed naturally required for a source of the gravitational field in the far zone. Put a bit more fancifully, this equation ensures the consistency of the coupling between short- and long-wavelength degrees of freedom.

The overline in the covariant derivative in (2.7) takes into account that this makes sense only when projected along the effective particle trajectory,

$$\overline{\nabla}_\mu = -\dot{X}_\mu \dot{X}^\nu \nabla_\nu. \quad (2.8)$$

Nevertheless the equation (2.7) has components both in directions orthogonal and parallel to the particle's velocity

$$(g_{\rho\nu} + \dot{X}_\rho \dot{X}_\nu) \overline{\nabla}_\mu T^{\mu\nu} = 0 \quad \Rightarrow \quad ma^\mu = 0, \quad (2.9)$$

$$\dot{X}_\nu \overline{\nabla}_\mu T^{\mu\nu} = 0 \quad \Rightarrow \quad \partial_\tau m(\tau) = 0, \quad (2.10)$$

with  $a^\mu = D_\tau \dot{X}^\mu = \dot{X}^\nu \nabla_\nu \dot{X}^\mu$  being the effective particle's acceleration. The first of these equations is the geodesic equation that determines the trajectory of a test particle.<sup>2</sup> The second equation implies that  $m$  is a constant along the trajectory.

Geodesic motion is so familiar that the effective theory for a black hole becomes of real interest only when it includes the corrections to the leading order equations [7]. In contrast, we will see that for black  $p$ -branes with  $p > 0$  the effective theory already yields non-trivial results at leading order. The method of matched asymptotic expansions (or the closely related classical effective theory of [9]) provides the conceptual backdrop to the blackfold approach, but at the practical level we will remain at the leading order approximation where the black brane is a 'test brane' in a background spacetime.

### 3 Effective blackfold theory

#### 3.1 Collective field variables

Our aim is to extend the effective worldline theory of black holes to a world-volume theory that describes the collective dynamics of a black  $p$ -brane.

<sup>2</sup> There is a long history of deriving the geodesic equation for a small particle (not necessarily a black hole) from the Einstein field equations, see [8] for a recent rigorous version. This can be taken as confirmation of our generic symmetry argument.

The geometry of a flat, static black  $p$ -brane in  $D$  spacetime dimensions is

$$ds^2 = - \left( 1 - \frac{r_0^n}{r^n} \right) dt^2 + \sum_{i=1}^p (dz^i)^2 + \frac{dr^2}{1 - \frac{r_0^n}{r^n}} + r^2 d\Omega_{n+1}^2. \quad (3.1)$$

Like in the previous example, the parameters of this solution include the ‘horizon thickness’  $r_0$  and the  $D - p - 1$  coordinates that parametrize the position of the brane in directions transverse to the worldvolume, which we denote collectively by  $X^\perp$  (making them explicit in the metric is possible but cumbersome). But now we must also include the possibility of a velocity  $u^i$  along the worldvolume of the brane. A covariant form of the boosted black brane metric is obtained by first introducing the coordinates  $\sigma^a = (t, z^i)$  that span the brane worldvolume with Minkowski metric  $\eta_{ab}$ , and a velocity  $u^a$  such that  $u^a u^b \eta_{ab} = -1$ . Then

$$ds^2 = \left( \eta_{ab} + \frac{r_0^n}{r^n} u_a u_b \right) d\sigma^a d\sigma^b + \frac{dr^2}{1 - \frac{r_0^n}{r^n}} + r^2 d\Omega_{n+1}^2. \quad (3.2)$$

Constant shifts of  $r_0$ , of  $u^i$ , and of  $X^\perp$  still give solutions to the Einstein equations. In total, these are  $D$  zero-modes that yield  $D$  collective coordinates of the black brane. The long-wavelength effective theory describes fluctuations in which these variables change slowly on the worldvolume  $\mathcal{W}_{p+1}$ , over a large length scale  $R \gg r_0$ . Typically  $R$  is set by the smallest extrinsic curvature radius of  $\mathcal{W}_{p+1}$ , or by the gradient of  $\ln r_0$  along the worldvolume. Background curvatures may also be present but they are usually already accounted for by the extrinsic curvature they induce on  $\mathcal{W}_{p+1}$ .

With this variation the worldvolume metric deviates from the Minkowski metric  $\eta_{ab}$ , and the near-zone geometry is of the form

$$ds^2 = \left( \gamma_{ab}(X^\mu(\sigma)) + \frac{r_0^n(\sigma)}{r^n} u_a(\sigma) u_b(\sigma) \right) d\sigma^a d\sigma^b + \frac{dr^2}{1 - \frac{r_0^n(\sigma)}{r^n}} + r^2 d\Omega_{n+1}^2 + \dots \quad (3.3)$$

where the dependence of  $\gamma_{ab}$  on the transverse coordinates gives rise to extrinsic curvature of the worldvolume, and the dots indicate that additional terms, of order  $O(r_0/R)$ , are required for this to be a solution to Einstein’s equations.<sup>3</sup>

When  $r \gg r_0$  this metric must match the geometry of the far-zone background with metric  $g_{\mu\nu}$ , in the region  $r \ll R$  around the worldvolume of an infinitely thin brane at  $x^\mu = X^\mu(\sigma)$ . Thus we identify  $\gamma_{ab}$  with the metric

<sup>3</sup> This is very similar to the long-wavelength perturbation of anti-deSitter black branes studied in [6].

induced on the effective brane worldvolume

$$\gamma_{ab} = g_{\mu\nu} \partial_a X^\mu \partial_b X^\nu. \quad (3.4)$$

Again, we are replacing the near-zone geometry with an infinitely thin  $p$ -brane, with worldvolume  $\mathcal{W}_{p+1}$ , embedded in the background geometry.

### 3.2 Effective stress-energy tensor

The stress-energy tensor of the black brane is, like the mass  $m$  of the black hole in the previous example, computed in the overlap region  $r_0 \ll r \ll R$  where the deviations away from Minkowski spacetime are small. It can be obtained as a generalization of the ADM mass, or equivalently, from the Brown-York quasilocal stress-energy tensor [10]. This is computed on a timelike surface with induced metric  $\tilde{h}_{\mu\nu}$  (not to be confused with  $h_{\mu\nu}$  below) and extrinsic curvature  $\Theta_{\mu\nu}$ , as

$$T_{\mu\nu}^{(ql)} = \frac{1}{8\pi G} \left( \Theta_{\mu\nu} - \tilde{h}_{\mu\nu} \Theta \right). \quad (3.5)$$

When measured at constant  $r \gg r_0$ , the divergent contributions to this tensor, which grow with  $r$ , can be subtracted in any of the conventional ways; for instance, the method of background subtraction from Minkowski space is enough for our purposes. Then, equivalently, this is the stress-energy tensor of a domain wall that encloses empty space and creates a field outside it equal to that of the black brane. This interpretation fits well with the idea that we replace the black brane with an effective source.

The surface at large constant  $r$  where the quasilocal  $T_{\mu\nu}^{(ql)}$  is computed has geometry  $\mathbb{R}^{1,p} \times S^{n+1}$ . We integrate it over the sphere to obtain the stress-energy tensor of the black  $p$ -brane

$$T_{ab} = \int_{S^{n+1}} T_{ab}^{(ql)}, \quad (3.6)$$

with components along the worldvolume directions.

For the boosted black  $p$ -brane (3.2) the result of this calculation is

$$T^{ab} = \frac{\Omega_{(n+1)}}{16\pi G} r_0^n \left( n u^a u^b - \eta^{ab} \right). \quad (3.7)$$

This is the stress-energy tensor of an isotropic perfect fluid,

$$T^{ab} = (\varepsilon + P) u^a u^b + P \eta^{ab}, \quad (3.8)$$

where the energy density  $\varepsilon$  and pressure  $P$  are

$$\varepsilon = \frac{\Omega_{(n+1)}}{16\pi G} (n+1) r_0^n, \quad P = -\frac{\Omega_{(n+1)}}{16\pi G} r_0^n. \quad (3.9)$$

In the rest frame of the fluid, and at any given point on the worldvolume, the Bekenstein-Hawking identification between horizon area and entropy applies to the black hole obtained by compactifying the  $p$  directions along the brane. Thus we identify an entropy density from the horizon area density of (3.1),

$$s = \frac{\Omega_{(n+1)}}{4G} r_0^{n+1}. \quad (3.10)$$

Locally, we also have the conventional relation between surface gravity and temperature

$$\mathcal{T} = \frac{n}{4\pi r_0}, \quad (3.11)$$

in such a way that the first law of black hole thermodynamics applies in the local form

$$d\varepsilon = \mathcal{T} ds. \quad (3.12)$$

In addition, the Euler-Gibbs-Duhem relation

$$\varepsilon + P = \mathcal{T} s \quad (3.13)$$

is verified.

After introducing a slow variation of the collective coordinates, the stress-energy tensor becomes

$$T^{ab}(\sigma) = \frac{\Omega_{(n+1)}}{16\pi G} r_0^n(\sigma) \left( n u^a(\sigma) u^b(\sigma) - \gamma^{ab}(\sigma) \right) + \dots \quad (3.14)$$

where the dots stand for terms with gradients of  $\ln r_0$ ,  $u^a$ , and  $\gamma_{ab}$ , responsible for dissipative effects that we are taking to be small. We neglect them for now, but will return to some of them in section 6.

### 3.3 Blackfold dynamics

In order to obtain the equations for the collective variables we need to recall a few notions about the geometry of worldvolume embeddings. More details and proofs are provided in the appendix.

#### *Worldvolume geometry*

The worldvolume  $\mathcal{W}_{p+1}$  is embedded in a background with metric  $g_{\mu\nu}$ , and its induced metric is (3.4). Indices  $\mu, \nu$  are raised and lowered with  $g_{\mu\nu}$ , and  $a, b$  with  $\gamma_{ab}$ . The first fundamental form of the submanifold

$$h^{\mu\nu} = \partial_a X^\mu \partial_b X^\nu \gamma^{ab} \quad (3.15)$$

acts as a projector onto  $\mathcal{W}_{p+1}$  (for a worldline,  $h^{\mu\nu} = -\dot{X}^\mu \dot{X}^\nu$ ), and the tensor

$$\perp_{\mu\nu} = g_{\mu\nu} - h_{\mu\nu} \quad (3.16)$$

projects along directions orthogonal to it.

Background tensors  $t^{\mu\dots\nu\dots}$  can be converted into worldvolume tensors  $t^{a\dots b\dots}$  and viceversa using the pull-back map  $\partial_a X^\mu$ , a relevant example being the stress-energy tensor

$$T^{\mu\nu} = \partial_a X^\mu \partial_b X^\nu T^{ab}. \quad (3.17)$$

The covariant differentiation of these background tensors is well defined only along tangential directions, which we denote by an overline,

$$\overline{\nabla}_\mu = h_\mu{}^\nu \nabla_\nu. \quad (3.18)$$

The divergence of the stress-energy tensor, projected parallel to  $\mathcal{W}_{p+1}$ , satisfies (see (A.9))

$$h^\rho{}_\nu \overline{\nabla}_\mu T^{\mu\nu} = \partial_b X^\rho D_a T^{ab}. \quad (3.19)$$

The *extrinsic curvature tensor*

$$K_{\mu\nu}{}^\rho = h_\mu{}^\sigma \overline{\nabla}_\nu h_{\sigma\rho} = -h_\mu{}^\sigma \overline{\nabla}_\nu \perp_{\sigma\rho} \quad (3.20)$$

is tangent to  $\mathcal{W}_{p+1}$  along its (symmetric) lower indices  $\mu, \nu$ , and orthogonal to  $\mathcal{W}_{p+1}$  along  $\rho$ . Its trace is the *mean curvature vector*

$$K^\rho = h^{\mu\nu} K_{\mu\nu}{}^\rho = \overline{\nabla}_\mu h^{\mu\rho}. \quad (3.21)$$

A useful result is that for any two vectors  $s^\mu$  and  $t^\mu$  tangent to  $\mathcal{W}_{p+1}$ ,

$$s^\mu t^\nu K_{\mu\nu}{}^\rho = \perp^\rho{}_\mu \nabla_s t^\mu = \perp^\rho{}_\mu \nabla_t s^\mu. \quad (3.22)$$

#### Blackfold equations

The classical dynamics of a generic brane has been studied by Carter in [11]. The equations are formulated in terms of a stress-energy tensor supported on, and tangent to, the  $p + 1$ -dimensional brane worldvolume  $\mathcal{W}_{p+1}$ ,

$$\perp^\rho{}_\mu T^{\mu\nu} = 0. \quad (3.23)$$

As in the example of  $p = 0$ , general covariance implies that the stress-energy tensor must obey the equations

$$\overline{\nabla}_\mu T^{\mu\rho} = 0. \quad (3.24)$$

This is a consequence of the underlying conservative dynamics of the full

General Relativity theory, but the effective worldvolume theory may be dissipative.

The divergence in (3.24) can be written as

$$\begin{aligned}\bar{\nabla}_\mu T^{\mu\rho} &= \bar{\nabla}_\mu(T^{\mu\nu}h_{\nu}{}^\rho) = T^{\mu\nu}\bar{\nabla}_\mu h_{\nu}{}^\rho + h_{\nu}{}^\rho\bar{\nabla}_\mu T^{\mu\nu} \\ &= T^{\mu\nu}K_{\mu\nu}{}^\rho + \partial_b X^\rho D_a T^{ab},\end{aligned}\tag{3.25}$$

where in the last line we used (3.19) and (3.20). Thus the  $D$  equations (3.24) separate into  $D - p - 1$  equations in directions orthogonal to  $\mathcal{W}_{p+1}$  and  $p + 1$  equations parallel to  $\mathcal{W}_{p+1}$ ,

$$T^{\mu\nu}K_{\mu\nu}{}^\rho = 0 \quad (\text{extrinsic equations}),\tag{3.26}$$

$$D_a T^{ab} = 0 \quad (\text{intrinsic equations}).\tag{3.27}$$

The extrinsic equations can be regarded as a generalization to  $p$ -branes of the geodesic equation (2.9) (where the acceleration is the extrinsic curvature of the worldline,  $a^\rho = -K^\rho$ ). In other words, this is the generalization of Newton's equation “mass  $\times$  acceleration = 0” to relativistic extended objects. The second set of equations, (3.27), express energy-momentum conservation on the worldvolume. For a black hole this was a rather trivial equation, but for a  $p$ -brane we get all the complexity of the hydrodynamics of a perfect fluid.

If we insert the stress-energy tensor of the black brane (3.7) and use (3.22), the extrinsic equations (3.26) become

$$K^\rho = n_\perp{}^\rho{}_\mu \dot{u}^\mu,\tag{3.28}$$

and the intrinsic equations (3.27),

$$\dot{u}_a + \frac{1}{n+1}u_a D_b u^b = \partial_a \ln r_0.\tag{3.29}$$

Here  $\dot{u}^\mu = u^\nu \nabla_\nu u^\mu$  and  $\dot{u}^b = u^c D_c u^b$ .

Eqs. (3.28) and (3.29) are the *blackfold equations*, a set of  $D$  equations that describe the dynamics of the  $D$  collective variables of a neutral black brane, in the approximation where we neglect its backreaction on the background (‘test brane’) as well as the dissipative effects on its worldvolume.

### 3.4 Blackfold boundaries

The worldvolume of the black  $p$ -brane may have boundaries specified by a function  $f(\sigma^a)$  such that  $f|_{\partial\mathcal{W}_{p+1}} = 0$ . If the effective fluid remains within these boundaries, the velocity must remain parallel to them,

$$u^a \partial_a f|_{\partial\mathcal{W}_{p+1}} = 0.\tag{3.30}$$

If the boundary is ‘free’, i.e., there is no surface tension, then the Euler (force) equations for a generic perfect fluid require that the pressure vanishes at the boundary. For the black brane this is

$$r_0|_{\partial\mathcal{W}_{p+1}} = 0. \quad (3.31)$$

Geometrically, this means that the horizon must approach zero size at the boundary, so the horizon closes off at the edge of the blackfold.

### 3.5 Blackfold as a black hole

The blackfold construction puts, on any point in the worldvolume  $\mathcal{W}_{p+1}$ , a (small) transverse sphere  $s^{n+1}$  with Schwarzschild radius  $r_0(\sigma)$ . If  $\mathcal{B}_p$  is a spatial section of  $\mathcal{W}_{p+1}$ , then the geometry of the horizon is the product of  $\mathcal{B}_p$  and  $s^{n+1}$  — the product is warped since the radius  $r_0(\sigma)$  of  $s^{n+1}$  varies along  $\mathcal{B}_p$ . If  $r_0$  is non-zero everywhere on  $\mathcal{B}_p$  then the  $s^{n+1}$  are trivially fibered on  $\mathcal{B}_p$  and the horizon topology is the product topology of  $\mathcal{B}_p$  and the sphere.

The regularity of this horizon in the perturbative expansion, in which it is distorted by long-wavelength fluctuations, is believed to be satisfied when the blackfold equations, which incorporate local thermodynamic equilibrium, are satisfied. A complete proof is still lacking, but refs. [12] and [13] provide evidence that this is true, respectively, for extrinsic and intrinsic deformations.

As we have seen, at boundaries of  $\mathcal{B}_p$  the size of  $s^{n+1}$  vanishes, so the horizon topology will be different. The regularity of the horizon at these boundaries is not fully understood yet and appears to depend on the specific type of boundary. We will return to this issue later.

## 4 Stationary blackfolds, action principle and thermodynamics

Equilibrium configurations for blackfolds that remain stationary in time are of particular interest since they correspond to stationary black holes. Requiring stationarity allows to solve explicitly the intrinsic equations for the thickness  $r_0$  and velocity  $u^a$ , so one is left only with the extrinsic equations for the worldvolume embedding  $X^\mu(\sigma)$ .

### 4.1 Solution to the intrinsic equations

For a fluid configuration to be stationary, dissipative effects must be absent. In general, this requires that the shear and expansion of its velocity field

$u$  vanish. One can then prove, using the fluid equations, that  $u$  must be proportional to a (worldvolume) Killing field  $k = k^a \partial_a$ . That is,

$$u = \frac{k}{|k|}, \quad |k| = \sqrt{-\gamma_{ab} k^a k^b} \quad (4.1)$$

where  $k$  satisfies the worldvolume Killing equation  $D_{(a} k_{b)} = 0$ . Actually, we will assume that this Killing vector on the worldvolume is the pull-back of a timelike Killing vector  $k^\mu \partial_\mu$  in the background,

$$\nabla_{(\mu} k_{\nu)} = 0, \quad (4.2)$$

such that  $k_a = \partial_a X^\mu k_\mu$ . The existence of this timelike Killing vector field is in fact a necessary assumption if we intend to describe stationary black holes.

The Killing equation (4.2) implies

$$\nabla_{(\mu} u_{\nu)} = -u_{(\mu} \nabla_{\nu)} \ln |k|, \quad (4.3)$$

so the acceleration is

$$\dot{u}^\mu = \partial^\mu \ln |k|. \quad (4.4)$$

Since the expansion of  $u$  vanishes, the intrinsic equation (3.29) becomes

$$\partial_a \ln |k| = \partial_a \ln r_0, \quad (4.5)$$

so

$$\frac{r_0}{|k|} = \text{constant}. \quad (4.6)$$

Expressed in terms of the local temperature  $\mathcal{T}$ , (3.11), this equation says that the worldvolume variation of the temperature is dictated by the local redshift factor  $|k|^{-1}$ ,

$$\mathcal{T}(\sigma) = \frac{T}{|k|}. \quad (4.7)$$

This result can also be derived for a general fluid using the equations of fluid dynamics. The integration constant  $T$  can be interpreted, using the thermodynamic first law that we derive below, as the global temperature of the black hole. Equation (4.6) can be read as saying that the thickness

$$r_0(\sigma) = \frac{n}{4\pi T} |k| \quad (4.8)$$

adjusts its value along the worldvolume so that  $T$  is a constant.

#### 4.2 Extrinsic equations and action for stationary blackfolds

With the intrinsic solutions (4.4) and (4.6), the extrinsic equations (3.28) reduce to

$$\begin{aligned} K^\rho &= n^\perp{}^{\rho\mu} \partial_\mu \ln r_0 \\ &= \perp^{\rho\mu} \partial_\mu \ln(-P). \end{aligned} \quad (4.9)$$

Using eq. (A.16) from the appendix, this equation can be equivalently found by varying, under deformations of the brane embedding, the action

$$I = \int_{\mathcal{W}_{p+1}} d^{p+1}\sigma \sqrt{-h} P. \quad (4.10)$$

This action, whose derivation actually need not assume any specific fluid equation of state, is a familiar one for branes with constant tension  $-P$ , whose worldvolume must be a minimal hypersurface so  $K^\rho = 0$  (an example are Dirac-Born-Infeld branes with zero gauge fields on their worldvolume). More generally, this is the action of a perfect fluid on  $\mathcal{W}_{p+1}$ .

Assume now that the background spacetime has a timelike Killing vector  $\xi$ , canonically normalized to generate unit time translations at asymptotic infinity, and whose norm on the worldvolume is

$$-\xi^2|_{\mathcal{W}_{p+1}} = R_0^2(\sigma). \quad (4.11)$$

Let us further assume that  $\xi$  is hypersurface-orthogonal, so we can foliate the blackfold in spacelike slices  $\mathcal{B}_p$  normal to  $\xi$ . The unit normal to  $\mathcal{B}_p$  is

$$n^a = \frac{1}{R_0} \xi^a. \quad (4.12)$$

$R_0$  measures the local gravitational redshift between worldvolume time and asymptotic time. Integrations over  $\mathcal{W}_{p+1}$  reduce, over an interval  $\Delta t$  of the Killing time generated by  $\xi$ , to integrals over  $\mathcal{B}_p$  with measure  $dV_{(p)}$ , so

$$I = \Delta t \int_{\mathcal{B}_p} dV_{(p)} R_0 P. \quad (4.13)$$

Using (4.8) in (3.9) we get an expression for the action in terms of  $k$  that is very practical for deriving the extrinsic equations in explicit cases,

$$\tilde{I}[X^\mu(\sigma)] = \int_{\mathcal{B}_p} dV_{(p)} R_0 |k|^n. \quad (4.14)$$

The tilde distinguishes it from (4.13), since we have removed an overall constant factor (including a sign) that is irrelevant for obtaining the equations.

### 4.3 Mass, angular momentum, entropy, and thermodynamics

Let  $k$  be given by a linear combination of orthogonal commuting Killing vectors of the background spacetime,

$$k = \xi + \sum_i \Omega_i \chi_i, \quad (4.15)$$

where  $\xi$  is the generator of time-translations that we introduced above, and  $\chi_i$  are generators of angular rotations in the background, normalized such that their orbits have periods  $2\pi$ . Then  $\Omega_i$  are the angular velocities of the blackfold along these directions.

The mass and angular momenta of the blackfold are now given by the integrals of the energy and momentum densities over  $\mathcal{B}_p$ ,

$$M = \int_{\mathcal{B}_p} dV_{(p)} T_{ab} n^a \xi^b, \quad J_i = - \int_{\mathcal{B}_p} dV_{(p)} T_{ab} n^a \chi_i^b. \quad (4.16)$$

The total entropy is deduced from the entropy current  $s^a = s(\sigma)u^a$ ,

$$S = - \int_{\mathcal{B}_p} dV_{(p)} s_a n^a = \int_{\mathcal{B}_p} dV_{(p)} \frac{R_0}{|k|} s(\sigma). \quad (4.17)$$

Let us now express the action (4.13) in terms of these quantities. Contracting the stress-energy tensor (3.8) with  $n_a k_b$ , then using (3.13) and (4.7), we find

$$T_{ab} n^a \left( \xi^b + \sum_i \Omega_i \chi_i^b \right) + T s u^a n_a = n^a k_a P = -R_0 P, \quad (4.18)$$

so, integrating over  $\mathcal{B}_p$ ,

$$I = -\Delta t \left( M - TS - \sum_i \Omega_i J_i \right). \quad (4.19)$$

This is an action in real Lorentzian time, but since we are dealing with time-independent configurations we can rotate to Euclidean time with periodicity  $1/T$  and recover the relation between the Euclidean action and the thermodynamic grand-canonical potential,  $I_E = W[T, \Omega_i]/T$ .

The identity (4.19) holds for any embedding, not necessarily a solution to the extrinsic equations, so if we regard  $M$ ,  $J_i$  and  $S$  as functionals of the  $X^\mu(\sigma)$  and consider variations where  $T$  and  $\Omega_i$  are held constant, we have

$$\frac{\delta I[X^\mu]}{\delta X^\mu} = 0 \quad \Leftrightarrow \quad \frac{\delta M}{\delta X^\mu} = T \frac{\delta S}{\delta X^\mu} + \sum_i \Omega_i \frac{\delta J_i}{\delta X^\mu}. \quad (4.20)$$

Therefore, the extrinsic equations are equivalent to the requirement that the first law of black hole thermodynamics holds for variations of the embedding.

Eq. (4.19), Wick-rotated to  $I_E[X^\mu]$ , is therefore an effective worldvolume action that approximates, to leading order in  $r_0/R$ , the Euclidean gravitational action of the black hole. One might have taken this thermodynamic effective action as the starting point for the theory of stationary blackfolds, but we have preferred to work with the equations of motion. These allow to consider situations away from stationary equilibrium and they also make more explicit the connection with worldvolume fluid dynamics.

Performing manipulations similar to (4.18) one finds that

$$(D-3)M - (D-2) \left( TS + \sum_i \Omega_i J_i \right) = \mathcal{T}_{\text{tot}}, \quad (4.21)$$

where

$$\mathcal{T}_{\text{tot}} = - \int_{\mathcal{B}_p} dV_{(p)} R_0 \left( \gamma^{ab} + n^a n^b \right) T_{ab} \quad (4.22)$$

is the total tensional energy, obtained by integrating the local tension over the blackfold volume.

The Smarr relation for asymptotically flat vacuum black holes in  $D$  dimensions [14],

$$(D-3)M - (D-2) \left( TS + \sum_i \Omega_i J_i \right) = 0 \quad (4.23)$$

must be recovered when the extrinsic equations for equilibrium are satisfied for a blackfold with compact  $\mathcal{B}_p$  in a Minkowski background where  $R_0 = 1$ . Thus, extrinsic equilibrium in Minkowski backgrounds implies

$$\mathcal{T}_{\text{tot}} = 0. \quad (4.24)$$

If the tensional energy did not vanish, it would imply the presence of sources of tension acting on the blackfold, e.g., in the form of conical or stronger singularities of the background space.

Another general identity is obtained by noticing that the blackfold fluid satisfies

$$-P = \frac{1}{n} \mathcal{T}_s. \quad (4.25)$$

Upon integration and using (4.19) we get

$$M - TS - \sum_i \Omega_i J_i = \frac{1}{n} TS, \quad (4.26)$$

or, in terms of the Euclidean action,  $I_E = S/n$ .

Note that while the thermodynamic form of the action (4.19) and the Smarr relation (4.23) are exactly valid for neutral black holes, eqs. (4.21) and (4.26) instead hold only to leading order in the expansion in  $r_0/R$ .

#### 4.4 Stationary blackfold boundaries

Let us now investigate what it means, for a stationary blackfold, that the thickness vanishes at its boundary, eq. (3.31).

In section 4.2 we have introduced the generators of unit time translations at asymptotic infinity,  $\xi^a$ , and on  $\mathcal{W}_{p+1}$ ,  $n^a$ , which are related by the factor  $R_0$  that measures the gravitational redshift between these two locations. On the other hand, relative to the worldvolume time generated by  $n^a$ , a fluid element on  $\mathcal{W}_{p+1}$  has a Lorentz-boost gamma factor equal to

$$-n^a u_a = \frac{1}{\sqrt{1-v^2}} \quad (4.27)$$

where  $v$  is the local fluid velocity,

$$v^2 = \sum_i v_i^2, \quad v_i = \frac{\Omega_i |\chi_i|}{R_0}. \quad (4.28)$$

Since the velocity  $u^a$  is determined by (4.1) and (4.15), then  $\xi^a u_a = \xi^a \xi_a / |k| = -R_0^2 / |k|$ , and

$$-n^a u_a = -\frac{1}{R_0} \xi^a u_a = \frac{R_0}{|k|}. \quad (4.29)$$

With (4.27), this implies

$$|k| = R_0 \sqrt{1-v^2}. \quad (4.30)$$

At a blackfold boundary we must have  $r_0 \rightarrow 0$ . According to (4.6), if the blackfold is stationary it must also be that  $|k| \rightarrow 0$ . There are two possibilities:

- (i)  $v \rightarrow 1$ : the fluid velocity becomes null at the boundary. There is some evidence that in this case the full horizon is smooth: as we will see in section 5.1, there are blackfolds with this kind of boundary for which we can compare to an exact black hole solution with a regular horizon.
- (ii)  $R_0 \rightarrow 0$ : the blackfold encounters a horizon of the background, where the gravitational redshift diverges. This boundary can be regarded as an intersection of horizons, and the evidence from known exact solutions indicates that the intersection point, i.e., the blackfold boundary, is singular.

Nevertheless, the evidence for these two behaviours is largely circumstantial and it would be desirable to have a better understanding of horizon regularity at blackfold boundaries.

#### 4.5 Ultraspinning behaviour

Let us assume that all length scales along  $\mathcal{B}_p$  are of the same order  $\sim R$  and that there are no large redshifts, of gravitational or Lorentz type, over most of the blackfold — this is naturally satisfied since the redshifts become large only near the boundaries. Then (setting temporarily  $G = 1$ ) eqs. (4.16) and (4.17) generically give

$$M \sim R^p r_0^n, \quad J \sim R^{p+1} r_0^n, \quad S \sim R^p r_0^{n+1}. \quad (4.31)$$

This implies

$$\frac{J}{M} \sim R, \quad (4.32)$$

so that neutral blackfolds are always in an ultraspinning regime, in which the angular momentum for fixed mass is very large. More precisely, in a neutral blackfold the length scale of angular-momentum (4.32) is always much larger than the length scale of the mass  $M^{1/(D-3)}$ ,

$$\frac{J/M}{M^{1/(D-3)}} \sim \left(\frac{r_0}{R}\right)^{\frac{D-p-3}{D-3}} \ll 1. \quad (4.33)$$

The entropy in (4.31) scales like

$$S(M, J) \sim J^{-\frac{p}{D-p-3}} M^{\frac{D-2}{D-p-3}}, \quad (4.34)$$

so, in dimension  $D$  and for fixed mass, the most entropic solution for a given number of large angular momenta  $J$  is attained by blackfolds with the smallest  $p$ . The intuitive reason is that, for a given mass, the horizon is thicker if  $p$  is smaller — the horizon spreads out less. A thicker horizon has lower temperature, and since  $TS \sim M$ , the entropy is higher. In section 5.3 we will find that there is always a black 1-fold for any number of angular momenta, which therefore maximizes the entropy.

## 5 Examples of blackfold solutions

This formalism can be applied easily to the explicit construction of stationary black holes. Besides finding new solutions, we will show that the blackfold method correctly recovers the limit in which known exact solutions become similar to black branes — these are the ultraspinning regime

of Myers-Perry black holes and the very-thin limit of the five-dimensional black ring, which provide non-trivial checks on the method.

### 5.1 Myers-Perry black hole as a blackfold disk

Myers-Perry black holes have ultraspinning regimes where the geometry near the rotation axis approaches that of a black brane spread along the rotation plane [15]. This suggests that these regimes may be reproduced by blackfold constructions, and indeed they are, in a rather non-trivial manner. Instead of studying the most general construction (see [4]), we will illustrate it in the case of the six-dimensional black hole rotating along a single plane, which already exhibits all the relevant features.

Take  $D = 6$  Minkowski spacetime as a background and a black 2-fold that extends along a plane within it (so  $n = 1$ ). The extrinsic equations are trivially solved, and we can restrict the analysis to the blackfold plane with polar coordinates  $(r, \phi)$  and metric

$$ds^2 = -dt^2 + dr^2 + r^2 d\phi^2. \quad (5.1)$$

We set the blackfold in rotation along  $\phi$ . Stationarity requires that the fluid rotates rigidly, eqs. (4.1) and (4.15) with  $\xi = \partial/\partial t$ ,  $\chi = \partial/\partial\phi$  and angular velocity  $\Omega$ , so the velocity is

$$u = \frac{1}{\sqrt{1 - \Omega^2 r^2}} \left( \frac{\partial}{\partial t} + \Omega \frac{\partial}{\partial \phi} \right). \quad (5.2)$$

The intrinsic equations are solved by appropriately redshifting the temperature, which determines the horizon thickness as in (4.8),

$$r_0(r) = \frac{1}{4\pi T} \sqrt{1 - \Omega^2 r^2}. \quad (5.3)$$

This implies that the extent of the blackfold along the rotation plane is limited to

$$0 \leq r \leq \Omega^{-1}. \quad (5.4)$$

Recall that according to eq. (3.31) the condition  $r_0(\Omega^{-1}) = 0$  specifies a boundary of the blackfold. The effective fluid velocity becomes lightlike there, and would be superluminal if we tried to go beyond this radius. Therefore the blackfold worldvolume is a disk.

It will be convenient to introduce two geometric parameters in place of  $T$  and  $\Omega$ : the disk radius  $a$ , and the blackfold thickness  $r_+$  at the rotation axis,

$$a = \Omega^{-1}, \quad r_+ = r_0(0) = \frac{1}{4\pi T}. \quad (5.5)$$

What is the topology of the horizon of this blackfold? The disk is fibered at each point with a sphere  $S^2$  of radius  $r_0(r)$  that shrinks to zero at the disk's edge. Topologically, this is  $S^4$ , i.e., the same as the topology of the horizon of the Myers-Perry black hole.

The mass and angular momentum of the blackfold are obtained from its energy and momentum densities,

$$T_{ab}n^a\xi^b = T_{tt} = \frac{r_+}{4G} \frac{2 - r^2/a^2}{\sqrt{1 - r^2/a^2}}, \quad (5.6)$$

$$-T_{ab}n^a\chi^b = T_{t\phi} = \frac{r_+}{4G} \frac{r^2/a}{\sqrt{1 - r^2/a^2}} \quad (5.7)$$

(since  $n^a = \xi^a$ ). Then

$$M = \int_0^{2\pi} d\phi \int_0^a dr r T_{tt} = \frac{2\pi}{3G} r_+ a^2, \quad (5.8)$$

$$J = \int_0^{2\pi} d\phi \int_0^a dr r T_{t\phi} = \frac{\pi}{3G} r_+ a^3. \quad (5.9)$$

The entropy-density current  $s^a = s u^a$  gives

$$-s^a n_a = \frac{\pi}{G} r_+^2 \sqrt{1 - r^2/a^2} \quad (5.10)$$

which integrates to

$$S = - \int_0^{2\pi} d\phi \int_0^a dr r s^a n_a = \frac{2\pi^2}{3G} r_+^2 a^2. \quad (5.11)$$

Let us now compare to the ultraspinning limit of the exact Myers-Perry black hole. This solution is specified by a mass parameter  $\mu$  and a rotation parameter  $a$ . The horizon radius  $r_+$  is obtained as the largest real root of

$$\mu = (r_+^2 + a^2)r_+. \quad (5.12)$$

In terms of these, the exact mass, spin and entropy are

$$M = \frac{2\pi}{3G} \mu, \quad J = \frac{1}{2} a M, \quad S = \frac{2\pi^2}{3G} r_+ \mu. \quad (5.13)$$

The ultraspinning regime of  $J \rightarrow \infty$  with fixed  $M$  is obtained as  $a \rightarrow \infty$ . In this limit eq. (5.12) becomes

$$\mu \rightarrow a^2 r_+, \quad (5.14)$$

and the physical quantities (5.13) become precisely the same as (5.8), (5.9), (5.11), after identifying the parameters  $r_+$  and  $a$  in both sides.

This identification of parameters is in fact geometrically meaningful. For an ultraspinning black hole the radii of the horizon in directions transverse and parallel to the rotation plane are [15]

$$r_{\perp}^{MP} \rightarrow r_+ \cos \theta, \quad r_{\parallel}^{MP} \rightarrow a, \quad (5.15)$$

where  $\theta$  is the polar angle on the horizon. For the blackfold disk, we have already seen that the radius in the plane parallel to the rotation is  $r_{\parallel}^{bf} = a$ . The square root in (5.3) suggests to introduce a polar angle  $\theta = \arcsin(r/a)$  such that the thickness of the blackfold in directions transverse to the rotation plane is

$$r_{\perp}^{bf} = r_0(r) = r_+ \cos \theta. \quad (5.16)$$

Identifying this polar angle with the one in the Myers-Perry solution, we find a perfect match between both sides.

Since the horizon of the Myers-Perry solution is smooth, this example yields evidence of regularity at the boundary of the blackfold where the fluid velocity becomes lightlike.

## 5.2 Curving black strings: black rings

We now consider stationary black 1-folds (i.e., curved black strings) in a Minkowski background

$$ds^2 = -dt^2 + dx_{(D-1)}^2 \quad (5.17)$$

with stationarity Killing vector  $\xi = \partial/\partial t$  so  $R_0 = 1$ .

Stationarity requires that the black string lies along a spatial Killing direction. Then the simplest way to solve the extrinsic equations is by imposing that the tensional energy vanishes, eq. (4.24). Since the string lies along an isometry, the integral in (4.22) is trivial and so the integrand, i.e., the tension measured relative to the frame defined by  $\xi$ , must vanish:

$$\text{tension} = - \left( \gamma^{ab} + \xi^a \xi^b \right) T_{ab} = 0. \quad (5.18)$$

Let us denote

$$- \xi^a u_a = \cosh \sigma \quad (5.19)$$

so  $\sigma$  is the rapidity that parametrizes the relative boost between the fluid and the background frame of observers along orbits of  $\xi$ . For a generic perfect fluid, the zero-tension condition (5.18) is

$$0 = \left( \gamma^{ab} + \xi^a \xi^b \right) \left( (\varepsilon + P) u_a u_b + P \gamma_{ab} \right) = \varepsilon \sinh^2 \sigma + P \cosh^2 \sigma \quad (5.20)$$

so at equilibrium the fluid velocity  $\tanh \sigma$  is fixed to the value

$$\tanh^2 \sigma = -\frac{P}{\varepsilon}. \quad (5.21)$$

Since  $-P/\varepsilon$  is actually the square of the velocity of transverse, elastic waves along the string, we see that the bending of the string can be regarded as the effect of supporting a stationary elastic wave along itself.

For the specific black string fluid (3.9), the condition (5.21) can be written as

$$\sinh^2 \sigma = \frac{1}{n}. \quad (5.22)$$

When  $n = 1$ , i.e., in  $D = 5$ , this is precisely the value for the boost that was found in [1] from the exact black ring solution in the limit where the ring is very thin and long,  $r_0/R \rightarrow 0$ . In this case the black string lies along a circle of radius  $R$  on a plane within  $\mathbb{R}^4$ .

It is straightforward to calculate (4.16) and (4.17) and check that, with this value of the boost, the blackfold construction reproduces all the physical magnitudes of the exact black ring solution to leading order in  $r_0/R$ . Beyond this order, ref. [12] has computed the first corrections to the metric, finding again perfect agreement with the perturbative expansion of the exact solution in  $D = 5$ , and checking that horizon regularity is preserved in any  $D \geq 5$ .

### 5.3 Helical black rings and minimal rigidity

The previous construction did not specify yet the geometry of the curve along which the string lies. However, as we saw, this must be along a spatial isometry of Euclidean space  $\mathbb{R}^{D-1}$ . If we are interested in blackfolds of finite extent, which correspond to asymptotically flat black objects, this isometry must be compact and therefore generated by rotational Killing vectors  $\partial/\partial\phi_i$ . This is, if we write the subspace of  $\mathbb{R}^{D-1}$  in which the embedding of the string is non-trivial as

$$ds^2 = \sum_{i=1}^m (dr_i^2 + r_i^2 d\phi_i^2), \quad (5.23)$$

then the string lies along the curve

$$r_i = R_i, \quad \phi_i = n_i \sigma, \quad 0 \leq \sigma < 2\pi. \quad (5.24)$$

An upper limit  $m \leq \lfloor \frac{D-1}{2} \rfloor = \lfloor \frac{n+3}{2} \rfloor$  is set by the rank of the spatial rotation group in  $D = n + 4$  spacetime dimensions. The  $D - 2m - 2$  dimensions of

space that are not explicit in (5.23) are totally orthogonal to the string and we will ignore them. They only play a role in providing, together with the  $m$  directions  $r_i$ , the  $n + 2$  dimensions orthogonal to the worldsheet in which the horizon of the black string is ‘thickened’ into a transverse  $s^{n+1}$  of radius  $r_0$ .

The  $n_i$  must be integers in order that the curve closes in on itself. Without loss of generality we assume  $n_i \geq 0$ . If we want to avoid multiple covering of the curve then the smallest of the  $n_i$  (which need not be unique), say  $n_1$ , must be coprime with all the  $n_i$ . Thus the set of  $n_i$  can be specified by  $m$  positive rational numbers  $n_i/n_1 \geq 1$ .

If all  $n_i = 1$  we obtain a circular planar ring along an orbit of  $\sum_i \partial_{\phi_i}$  with radius  $\sqrt{\sum_i R_i^2}$ . If, instead, at least two  $n_i$  are non-zero and not both equal to one then we obtain *helical black rings*. Together with planar black rings, this exhausts all possible stationary black 1-folds in a Minkowski background with a spatially compact worldsheet.

The Killing generator of the worldsheet velocity field is

$$k = \frac{\partial}{\partial t} + \sum_i \Omega_i \frac{\partial}{\partial \phi_i}, \quad (5.25)$$

where the ratios between angular velocities must be rational

$$\left| \frac{\Omega_i}{\Omega_j} \right| = \frac{n_i}{n_j} \quad \forall i, j, \quad (5.26)$$

and the equilibrium condition (5.22) fixes

$$\sum_{i=1}^m \Omega_i^2 R_i^2 = \frac{1}{n+1}. \quad (5.27)$$

The physical properties (mass, spins, entropy etc) of helical black rings in the approximation  $r_0/R_i \ll 1$  are computed in [4]. One finds that helical black rings are the solutions with the largest entropy among all blackfolds with given values of the mass and angular momenta. Among helical black rings, the maximal entropy for a given set of values of the angular momenta is achieved by minimizing the  $n_i$ , since this makes the ring shorter and hence thicker. For a single angular momentum, the planar black ring maximizes the entropy.

*Maximal symmetry breaking and saturation of the rigidity theorem*

A spacetime containing a helical ring has the isometry generated by

$$\sum_i n_i \frac{\partial}{\partial \phi_i} \quad (5.28)$$

along the direction of the string. However, this string breaks in general other  $U(1)$  isometries of the background, possibly leaving (5.28) as the only spatial Killing vector of the configuration.

In order to prove this point, observe that any additional  $U(1)$  symmetry must leave the curve invariant, i.e., the curve must lie at a fixed point of the isometry. This is, the curve must be on a point in some plane in  $\mathbb{R}^{D-1}$ , so rotations in this plane around the point leave it invariant. Let us parametrize the most general possible helical curve in  $\mathbb{R}^{D-1}$  as a curve in  $\mathbb{C}^m$ , with  $m = \lfloor \frac{D-1}{2} \rfloor$ , of the form

$$z_i = R_i e^{in_i \sigma}, \quad (5.29)$$

where possibly some of the  $n_i$  are zero. In order to find a plane in which rotations leave the curve invariant we must solve the equation

$$\sum_{i=1}^m a_i z_i = 0 \quad (5.30)$$

with complex  $a_i$ , for all values of  $\sigma$ . This equation admits a non-trivial solution only if some of the  $n_i$  are equal to each other (possibly zero).

Therefore, if (i) the string circles around in all of the  $m = \lfloor \frac{D-1}{2} \rfloor$  independent rotation planes, i.e., all the possible  $n_i$  are non-zero, and (ii) all the  $n_i$ 's are different from each other, then the only spatial Killing vector of the configuration is (5.28). In this case, we obtain an asymptotically flat helical black ring with only one spatial  $U(1)$  isometry.

The black hole rigidity theorem of [16, 17] requires that stationary non-static black holes have at least one such isometry, and ref. [18] had conjectured that black holes exist with not more than this symmetry. The construction of helical black rings that rotate in all possible planes and have exactly one spatial  $U(1)$  proves this conjecture in any  $D \geq 5$ .

#### 5.4 Odd-spheres

For our final example, we describe a large family of solutions for black holes in  $D$ -dimensional flat space with horizon topology

$$\left( \prod_{p_a=\text{odd}} S^{p_a} \right) \times s^{n+1}, \quad \sum_{a=1}^{\ell} p_a = p. \quad (5.31)$$

In this case, the spatial section of the blackfold worldvolume  $\mathcal{B}_p$  is a product of odd-spheres.

##### $S^{2k+1}$ blackfolds

We consider first a single odd-sphere  $S^{2k+1}$ , which contains the black ring as the particular case  $k = 0$ . We embed the sphere  $S^{2k+1}$  into a  $(2k + 2)$ -dimensional flat subspace of  $\mathbb{R}^{D-1}$  with metric

$$dr^2 + r^2 d\Omega_{2k+1}^2. \quad (5.32)$$

The unit metric on  $S^{2k+1}$  can be written as

$$d\Omega_{2k+1}^2 = \sum_{i=1}^{k+1} (d\mu_i^2 + \mu_i^2 d\phi_i^2), \quad \sum_{i=1}^{k+1} \mu_i^2 = 1, \quad (5.33)$$

where  $\phi_i$  are the angles that parametrize the Cartan subgroup of the rotation group  $SO(2k + 2)$ .

In the general stationary case we would consider the blackfold embedded as  $r = R(\mu_1, \dots, \mu_k)$ . Then the extrinsic equations give a set of differential equations for  $R(\mu_i)$  involving  $k$  angular velocities  $\Omega_i$ . These are complicated to solve, but they simplify to algebraic equations in the still non-trivial instance that the sphere is geometrically round with constant radius  $r = R$ , and rotates with the same angular velocity  $\Omega$  in all angles. Then the stationarity Killing vector is

$$k = \frac{\partial}{\partial t} + \Omega \sum_{i=1}^{k+1} \frac{\partial}{\partial \phi_i}, \quad |k| = \sqrt{1 - \Omega^2 R^2}, \quad (5.34)$$

and the blackfold is homogeneous so the thickness  $r_0$  is constant over the worldvolume.

The extrinsic equations for  $R$  can be easily (and consistently) obtained from the stationary blackfold action (4.14)

$$\tilde{I}[R] = \Omega_{(p)} R^p (1 - R^2 \Omega^2)^{\frac{n}{2}}, \quad p = 2k + 1. \quad (5.35)$$

This is extremized when

$$R = \frac{1}{\Omega} \sqrt{\frac{p}{n+p}}. \quad (5.36)$$

Equivalently, this value makes the local tension (5.18) vanish at each point. When  $p = 1$  we recover the result for black rings. Having this equilibrium radius of round blackfolds, it is straightforward to compute their physical properties [4].

### Products of odd-spheres

This construction can be easily extended to solutions where  $\mathcal{B}_p$  is a product of round odd-spheres, each one labeled by an index  $a = 1, \dots, \ell$ . Denoting the radius of the  $S^{p_a}$  factor ( $p_a = \text{odd}$ ) by  $R_a$  we take the angular momenta of the  $a$ -th sphere to be all equal to  $\Omega^{(a)}$ .

We embed the product of  $\ell$  odd-spheres in a flat  $(p + \ell)$ -dimensional subspace of  $\mathbb{R}^{D-1}$  with metric

$$\sum_{a=1}^{\ell} \left( dr_a^2 + r_a^2 d\Omega_{(p_a)}^2 \right), \quad \sum_{a=1}^{\ell} p_a = p \quad (5.37)$$

and locate the blackfold at  $r_a = R_a$ . Note that given a value of  $n = D - p - 3 \geq 1$ , the number  $\ell$  of spheres in the product is limited to  $\ell \leq n + 2$ .

With the spheres being geometrically round, the stationary blackfold action (4.14) reduces to

$$\tilde{I}[R_a] = \prod_{b=1}^{\ell} \Omega_{(p_b)} R_b^{p_b} \left( 1 - \sum_{a=1}^{\ell} \left( R_a \Omega^{(a)} \right)^2 \right)^{n/2}, \quad (5.38)$$

whose variation with respect to each of the  $R_a$ 's gives the equilibrium conditions

$$R_a = \frac{1}{\Omega^{(a)}} \sqrt{\frac{p_a}{n+p}}. \quad (5.39)$$

A simple case is the  $p$ -torus, where we set all  $p_a = 1$ . This gives black holes with horizon topology  $\mathbb{T}^p \times s^{n+1}$  that rotate simultaneously along all orthogonal one-cycles of  $\mathbb{T}^p$ .

It is easy to see that, like the Myers-Perry black holes and the planar black rings, these odd-sphere solutions do not break any of the commuting isometries of the background.

To finish this section we note that, except for the case of black 1-folds, our analysis has not been systematic enough to be complete, and further classes of black holes can be expected in  $D \geq 6$ . But already with the ones we

have presented, one can easily see that black hole uniqueness is very badly violated in higher-dimensions.

## 6 Gregory-Laflamme instability and black brane viscosity

The blackfold approach must capture the perturbative dynamics of a black hole when the perturbation along the horizon has long wavelength  $\lambda$ ,

$$\lambda \gg r_0. \quad (6.1)$$

This includes in particular intrinsic fluctuations of the black brane in which the worldvolume geometry remains flat but  $r_0$  and  $u^a$  are allowed to vary. A variation of the thickness of the brane,  $\delta r_0$ , is a variation of the pressure and density of the effective fluid. Then, for small fluctuations we expect to recover sound waves along the brane. These turn out to be unstable in an interesting way.

### 6.1 Sound waves on a black brane

Sound waves are easily derived for a generic perfect fluid. Introduce small perturbations in an initial uniform state at rest,

$$\varepsilon \rightarrow \varepsilon + \delta\varepsilon, \quad P \rightarrow P + \frac{dP}{d\varepsilon}\delta\varepsilon, \quad u^a = (1, 0 \dots) \rightarrow (1, \delta u^i). \quad (6.2)$$

To linear order in the perturbations the intrinsic fluid equations (3.27) give

$$\left( \partial_t^2 - \frac{dP}{d\varepsilon} \partial_i^2 \right) \delta\varepsilon = 0, \quad (6.3)$$

so longitudinal, sound-mode oscillations of the fluid propagate with squared speed

$$v_s^2 = \frac{dP}{d\varepsilon}. \quad (6.4)$$

Neutral blackfolds have imaginary speed of sound

$$v_s^2 = -\frac{1}{n+1}, \quad (6.5)$$

which implies that sound waves along the effective black brane fluid are unstable: under a density perturbation the fluid evolves to become more and more inhomogeneous. Thus the black brane horizon itself becomes inhomogeneous, with the brane thickness  $r_0$  varying along the brane as

$$\delta r_0 \sim e^{\Omega t + i k_i z^i}, \quad (6.6)$$

with

$$\Omega = \frac{k}{\sqrt{n+1}} + O(k^2). \quad (6.7)$$

( $k = \sqrt{k_i k_i}$ ). Unstable oscillations of the form (6.6) are the type of black brane instability discovered by Gregory and Laflamme (see [5]). Using the blackfold effective theory, we have derived it in the regime of long wavelengths,  $kr_0 \ll 1$ . Many studies of the Gregory-Laflamme instability focus on the threshold mode, with  $\Omega = 0$  at  $k = k_{GL} \neq 0$ , which has ‘small’ wavelength  $2\pi/k_{GL} \sim r_0$  and typically needs numerical work to determine. The blackfold approach instead reveals that the hydrodynamic modes, which have vanishing frequency as  $k \rightarrow 0$ , are much simpler to study. The slope of the curve  $\Omega(k)$  near  $k = 0$  is exactly determined using only the equation of state  $P(\varepsilon)$  of the unperturbed, static black brane.

### 6.2 Correlated dynamical and thermodynamical stability

It is conventional in fluid dynamics to express the speed of sound in terms of thermodynamic quantities. Using the Gibbs-Duhem relation  $dP = sd\mathcal{T}$  one finds

$$\frac{dP}{d\varepsilon} = s \frac{d\mathcal{T}}{d\varepsilon} = \frac{s}{c_v}, \quad (6.8)$$

where  $c_v$  is the isovolumetric specific heat. So the black brane is dynamically unstable to long wavelength, hydrodynamical perturbations, if and only if it is locally thermodynamically unstable,  $c_v < 0$ . The ‘correlated stability conjecture’ of Gubser and Mitra [19] posits precisely this type of connection between dynamical and thermodynamic stability. The blackfold method not only shows very simply why it holds for hydrodynamic modes, but it also gives a quantitative expression for the unstable frequency in terms of local thermodynamics as

$$\Omega = \sqrt{\frac{s}{-c_v}} k + O(k^2). \quad (6.9)$$

### 6.3 Viscous damping

The previous analysis of the sound-wave instability employed the stress-energy tensor of eq. (3.7), which gives the perfect fluid approximation to the intrinsic dynamics of the black brane. This tensor was obtained from the stationary metric of the black brane. If we perturb this brane, it will vibrate

in its quasinormal modes, with damped oscillations. The stress-energy tensor measured at large distance  $r \gg r_0$  from the black  $p$ -brane will reflect this damping through the appearance of dissipative terms, proportional to derivatives of  $u^a$  (the derivatives of  $r_0$  are proportional to these), so that

$$T_{ab} = T_{ab}^{(perfect)} - \zeta \theta P_{ab} - 2\eta \sigma_{ab} + O(D^2). \quad (6.10)$$

Here the orthogonal projector, expansion and shear of the velocity congruence are

$$P_{ab} = \eta_{ab} + u_a u_b, \quad \theta = D_a u^a, \quad (6.11)$$

$$\sigma_{ab} = P_a^c P_b^d \left( D_{(c} u_{d)} - \frac{1}{p} \theta P_{cd} \right), \quad (6.12)$$

and the coefficients  $\eta$  and  $\zeta$  are the effective shear and bulk viscosity of the black brane. They can be computed from a perturbative calculation very similar to those in the context of the fluid/AdS-gravity correspondence of [6]. For the neutral black brane in asymptotically flat space this calculation has been carried out in [13], with the result that

$$\eta = \frac{s}{4\pi}, \quad \zeta = \frac{s}{2\pi} \left( \frac{1}{p} - v_s^2 \right), \quad (6.13)$$

where  $s$  is the entropy density of the black brane (3.10) and  $v_s$  the speed of sound (6.5).

Now we can solve the fluid equations (3.27) for linearized sound-mode perturbations of the viscous fluid, and obtain the leading corrections to the dispersion relation (6.7) at order  $k^2$ . For the black brane fluid the result is

$$\Omega = \frac{k}{\sqrt{n+1}} \left( 1 - \frac{n+2}{n\sqrt{n+1}} k r_0 \right), \quad (6.14)$$

which is valid up to corrections  $O(k^3)$ . We see that viscosity has the expected effect of damping the sound waves. Figure 1. compares this dispersion relation to the numerical results obtained by solving the linearized perturbations of a black string.

Eq. (6.14) gives excellent agreement to the numerical data for small  $k r_0$ , but it also shows a remarkable overall resemblance to them even when  $k r_0$  is of order one, which is beyond the expected range of validity of the approximation. The quantitative agreement improves with increasing  $n$ : in an expansion in  $1/n$ , eq. (6.14) obtains the exact leading-order value for the threshold wavenumber  $k_{GL} \rightarrow \sqrt{n}/r_0$ . Ref. [13] suggests to explain this surprising agreement by noting that the thermal wavelength  $\lambda_T = 1/T \sim r_0/n$

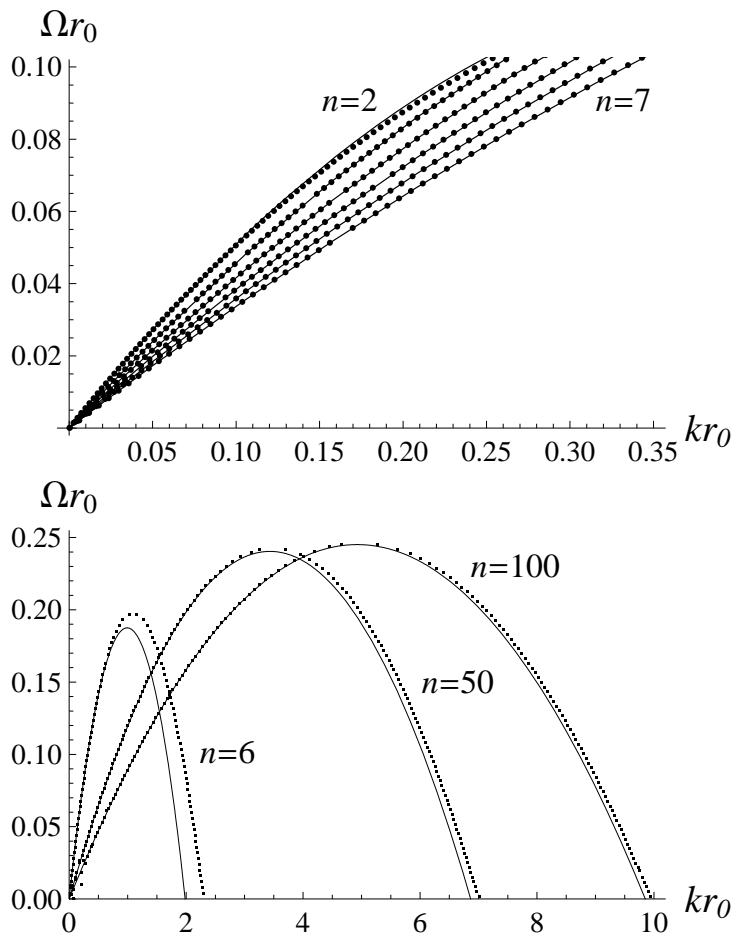


Figure 1.  $\Omega(k)$  for unstable modes of black  $p$ -branes, in units of  $1/r_0$  (the results depend only on  $n$  in (1.1)). The continuous curves are the analytical approximation (6.14), the dots are the numerical solution of the perturbations of black branes. The top diagram shows results for  $n = 2, \dots, 7$  at small  $k$ . The bottom diagram shows the curves for  $n = 6, 50, 100$  at all  $k$ . For large  $n$ , eq. (6.14) underestimates the wavenumber of the threshold mode by only  $1/n$ .

shrinks to zero as  $n \rightarrow \infty$  for fixed  $r_0$ . Quite plausibly, this effect extends the range of wavelengths that fall under the remit of fluid dynamics.

Let us emphasize how little has gone into the derivation of (6.14): only the equation of state  $P(\varepsilon)$  and the viscosities  $\eta$  and  $\zeta$  — actually, for a black string there is only  $\zeta$ . The determination of these coefficients requires a study of perturbations of the black string, but this can be carried out analytically

for all  $n$  and  $p$  and needs to be done only once. Furthermore, the result for  $\eta$  is known to be universal for black holes, and the value of  $\zeta$  saturates a proposed bound [20] which may plausibly be proven in generality. If there exists such a general argument for the value of  $\zeta$  for a black brane, then the entire expression for the curve (6.14) can be obtained, using simple algebra, from knowledge of only  $dP/d\varepsilon$ .

Thus, the effective viscous fluid of the blackfold approach seems to capture in a strikingly simple manner some of the most characteristic features of black brane dynamics. This is a significant simplification of the complexity of Einstein's equations.

## 7 Extensions

Although in section 5 we have only considered Minkowski backgrounds, the effective theory of blackfolds can be readily applied to the construction of black holes in curved backgrounds, such as deSitter or anti-deSitter spacetime with cosmological constant  $\Lambda$ . In this case it is necessary that the thickness  $r_0$  be much smaller than the curvature radius  $|\Lambda|^{-1/2}$ , so the vacuum black brane solution can be a good approximation in the near-zone. Black rings, odd-spheres, and other blackfolds with characteristic radii  $R$  that can be larger or smaller than  $|\Lambda|^{-1/2}$ , are easy to construct in these spacetimes [21, 22], as well as in other non-trivial backgrounds such as Kaluza-Klein monopoles [23].

Black  $p$ -branes can also carry on their worldvolumes the charges of  $q$ -branes,  $0 \leq q \leq p$ , which are sources of  $(q+2)$ -form gauge field strengths  $F_{q+2}$  [24, 25]. Then the worldvolume fluid includes a conserved  $q$ -brane number current. For  $q = 0$  this is a theory of an isotropic fluid with a conserved particle number, but when  $q \geq 1$  the brane current makes the fluid anisotropic.

Blackfolds with a spatially compact worldvolume that supports these currents correspond to black holes that source the field  $F_{q+2}$ . When  $q = 0$  they carry a conserved charge of a Maxwell field. When  $q \geq 1$  they carry a dipole of the field. In contrast to neutral blackfolds, black holes constructed as charged blackfolds need not be ultraspinning: the rotation may be small if the charge of the black brane is close to its upper extremal limit. The presence of charge close to extremality can also eliminate, in certain cases, the Gregory-Laflamme instability of the black brane. Then, the black holes that result may be dynamically stable.

Of particular interest for string theory are blackfolds that carry Ramond-Ramond charges. In general, blackfold techniques are an appropriate tool for the study of configurations of D-branes in the probe approximation, in

the case that the D-brane worldvolume theory has a thermal population of excitations. The blackfold gives a gravitational description of this thermally excited worldvolume, with a horizon that on short scales is like that of the straight black D-brane. Like in the AdS/CFT correspondence, this gravitational description of the worldvolume theory is appropriate when there is a stack of a large number of D-branes (although not so large as to cause a strong backreaction on the background) and the theory is strongly coupled. Ref. [26] develops these methods to study a thermal version of the D3-brane bion.

### **Acknowledgments**

I am indebted to my collaborators in the development of the blackfold approach: Marco Caldarelli, Joan Camps, Nidal Haddad, Troels Harmark, Vasilis Niarchos, Niels Obers, María J. Rodríguez. I also thank Pau Figueras for the numerical data used in figure 1. Work supported by MEC FPA2010-20807-C02-02, AGAUR 2009-SGR-168 and CPAN CSD2007-00042 Consolider-Ingenio 2010

## Appendix: Geometry of submanifolds

### A.1 Extrinsic curvature

For a submanifold  $\mathcal{W}$  embedded as  $X^\mu(\sigma^a)$ , the pull-back of the spacetime metric onto  $\mathcal{W}$ ,  $\gamma_{ab}$ , is (3.4) and the first fundamental form of the surface,  $h_{\mu\nu}$ , is obtained as eq. (3.15). It satisfies

$$h^\mu{}_\nu \partial_a X^\nu = \partial_a X^\mu, \quad h^\mu{}_\nu h^\nu{}_\rho = h^\mu{}_\rho, \quad (\text{A.1})$$

so  $h^\mu{}_\nu$  projects tensors onto directions tangent to  $\mathcal{W}$ .  $\perp_{\mu\nu}$ , introduced in (3.16), projects onto orthogonal directions,

$$\perp_{\mu\nu} \partial_a X^\mu = 0, \quad \perp_\mu{}^\nu \perp_\nu{}^\rho = \perp_\mu{}^\rho. \quad (\text{A.2})$$

The shape of the embedding of the submanifold  $\mathcal{W}$  is captured by the second fundamental tensor, or extrinsic curvature tensor, (3.20). Symmetry of the first two indices of  $K_{\mu\nu}{}^\rho$  is equivalent to the integrability of the subspaces orthogonal to  $\perp_\mu{}^\nu$ . To see this, let  $s$  and  $t$  be any two vectors in this subspace,

$$\perp^\mu{}_\nu t^\nu = 0, \quad \perp^\mu{}_\nu s^\nu = 0. \quad (\text{A.3})$$

Then one can easily prove from the definition of  $K_{\mu\nu}{}^\rho$  that

$$s^\mu t^\nu K_{\mu\nu}{}^\rho = \perp^\rho{}_\mu \nabla_s t^\mu, \quad (\text{A.4})$$

so

$$K_{[\mu\nu]}{}^\rho = 0 \Leftrightarrow 0 = \perp^\rho{}_\mu (\nabla_s t^\mu - \nabla_t s^\mu) = \perp^\rho{}_\mu [s, t]^\mu. \quad (\text{A.5})$$

The vanishing of the last commutator is equivalent, though Frobenius' theorem, to the integrability of the subspace orthogonal to  $\perp_\mu{}^\nu$ . Therefore the extrinsic curvature tensor of the submanifold  $\mathcal{W}$  satisfies  $K_{[\mu\nu]}{}^\rho = 0$ .

Now let  $N$  be any vector orthogonal to  $\mathcal{W}$ . Then

$$N_\rho K_{\mu\nu}{}^\rho = N_\rho h_\nu{}^\sigma \bar{\nabla}_\mu h_{\sigma\rho} = -h_\nu{}^\rho \bar{\nabla}_\mu N_\rho. \quad (\text{A.6})$$

Background tensors  $t_{\mu_1\mu_2\dots}{}^{\nu_1\nu_2\dots}$  can be pulled-back onto worldvolume tensors  $t_{a_1a_2\dots}{}^{b_1b_2\dots}$  using  $\partial_a X^\mu$  as

$$t_{a_1a_2\dots}{}^{b_1b_2\dots} = \partial_{a_1} X^{\mu_1} \partial_{a_2} X^{\mu_2} \dots \partial^{b_1} X_{\nu_1} \partial^{b_2} X_{\nu_2} \dots t_{\mu_1\mu_2\dots}{}^{\nu_1\nu_2\dots}, \quad (\text{A.7})$$

where

$$\partial^b X_\nu = \gamma^{bc} h_{\nu\rho} \partial_c X^\rho. \quad (\text{A.8})$$

Even when  $t_{\mu_1\mu_2\dots}{}^{\nu_1\nu_2\dots}$  has all indices parallel to  $\mathcal{W}$ , in general  $\bar{\nabla}_\mu t_{\mu_1\mu_2\dots}{}^{\nu_1\nu_2\dots}$  has both parallel and orthogonal components. The parallel projection along all indices is related to the worldvolume covariant derivative  $D_a t_{a_1a_2\dots}{}^{b_1b_2\dots}$

as in (A.7). Then, the divergences of background and worldvolume tensors are related as

$$h^{\nu_1}{}_{\mu_1} \dots \bar{\nabla}_\rho t^{\rho\mu_1\dots} = \partial_{a_1} X^{\nu_1} \dots D_c t^{ca_1\dots}. \quad (\text{A.9})$$

### A.2 Variational calculus

Consider a congruence of curves with tangent vector  $N$ , that intersect  $\mathcal{W}$  orthogonally

$$N^\mu h_{\mu\nu} = 0, \quad N^\mu \perp_{\mu\nu} = N_\nu, \quad (\text{A.10})$$

and Lie-drag  $\mathcal{W}$  along these curves. The congruence is arbitrary, other than requiring it to be smooth in a finite neighbourhood of  $\mathcal{W}$ , so this realizes arbitrary smooth deformations of the worldvolume  $X^\mu \rightarrow X^\mu + N^\mu$ .

Consider now the Lie derivative of  $h_{\mu\nu}$  along  $N$ . In general,

$$\mathcal{L}_N h_{\mu\nu} = N^\rho \nabla_\rho h_{\mu\nu} + h_{\rho\nu} \nabla_\mu N^\rho + h_{\mu\rho} \nabla_\nu N^\rho. \quad (\text{A.11})$$

Using (A.6) one can derive

$$N_\rho K_{\mu\nu}{}^\rho = -\frac{1}{2} h_\mu{}^\lambda h_\nu{}^\sigma \mathcal{L}_N h_{\lambda\sigma}. \quad (\text{A.12})$$

Taking the trace,

$$N_\rho K^\rho = -\frac{1}{2} h^{\mu\nu} \mathcal{L}_N h_{\mu\nu} = -\frac{1}{\sqrt{|h|}} \mathcal{L}_N \sqrt{|h|}, \quad (\text{A.13})$$

where  $h = \det h_{\mu\nu}$ . These equations generalize well-known expressions for the extrinsic curvature of a codimension-1 surface.

Consider now a functional of the embedding of the form

$$I = \int_{\mathcal{W}} \sqrt{|h|} \Phi \quad (\text{A.14})$$

where  $\Phi$  is a worldvolume function. Then

$$\delta_N I = \mathcal{L}_N (\sqrt{|h|} \Phi) = \sqrt{|h|} (-N_\rho K^\rho \Phi + N^\rho \partial_\rho \Phi). \quad (\text{A.15})$$

Since  $N$  is an arbitrary orthogonal vector we have

$$\delta_N I = 0 \quad \Leftrightarrow \quad K^\rho = \perp^{\rho\mu} \partial_\mu \ln \Phi. \quad (\text{A.16})$$

If  $\Phi$  is constant then we recover the equation  $K^\rho = 0$  for minimal-volume submanifolds.

## References

- [1] R. Emparan and H. S. Reall, “Black rings,” chapter of this book.
- [2] R. Emparan, T. Harmark, V. Niarchos and N. A. Obers, “World-volume effective theory for higher-dimensional black holes. (Blackfolds),” *Phys. Rev. Lett.* **102**, 191301 (2009) [arXiv:0902.0427 [hep-th]].
- [3] R. Emparan, T. Harmark, V. Niarchos and N. A. Obers, “Essentials of Blackfold Dynamics,” *JHEP* **1003** (2010) 063 [arXiv:0910.1601 [hep-th]].
- [4] R. Emparan, T. Harmark, V. Niarchos and N. A. Obers, “New Horizons for Black Holes and Branes,” *JHEP* **1004** (2010) 046 [arXiv:0912.2352 [hep-th]].
- [5] R. Gregory, “Gregory-Laflamme instability,” chapter of this book.
- [6] V. Hubeny, M. Rangamani, S. Minwalla, “Gravity/fluid correspondence,” chapter of this book.
- [7] E. Poisson, “The motion of point particles in curved spacetime,” *Living Rev. Rel.* **7**, 6 (2004) [arXiv:gr-qc/0306052].
- [8] S. E. Gralla and R. M. Wald, “A Rigorous Derivation of Gravitational Self-force,” *Class. Quant. Grav.* **25** (2008) 205009 [arXiv:0806.3293 [gr-qc]].
- [9] W. D. Goldberger and I. Z. Rothstein, “An effective field theory of gravity for extended objects,” *Phys. Rev. D* **73**, 104029 (2006) [arXiv:hep-th/0409156].
- [10] J. D. Brown and J. W. York, “Quasilocal energy and conserved charges derived from the gravitational action,” *Phys. Rev. D* **47**, 1407 (1993) [arXiv:gr-qc/9209012].
- [11] B. Carter, “Essentials of classical brane dynamics,” *Int. J. Theor. Phys.* **40**, 2099 (2001) [arXiv:gr-qc/0012036].
- [12] R. Emparan, T. Harmark, V. Niarchos, N. A. Obers and M. J. Rodríguez, “The Phase Structure of Higher-Dimensional Black Rings and Black Holes,” *JHEP* **0710**, 110 (2007) [arXiv:0708.2181 [hep-th]].
- [13] J. Camps, R. Emparan and N. Haddad, “Black Brane Viscosity and the Gregory-Laflamme Instability,” *JHEP* **1005** (2010) 042 [arXiv:1003.3636 [hep-th]].
- [14] T. Harmark, N. A. Obers, “New phase diagram for black holes and strings on cylinders,” *Class. Quant. Grav.* **21** (2004) 1709. [hep-th/0309116].
- [15] R. Emparan and R. C. Myers, “Instability of ultra-spinning black holes,” *JHEP* **0309** (2003) 025 [arXiv:hep-th/0308056].
- [16] S. Hollands, A. Ishibashi and R. M. Wald, “A Higher Dimensional Stationary Rotating Black Hole Must be Axisymmetric,” *Commun. Math. Phys.* **271**, 699 (2007) [arXiv:gr-qc/0605106].

- [17] V. Moncrief and J. Isenberg, “Symmetries of Higher Dimensional Black Holes,” *Class. Quant. Grav.* **25** (2008) 195015. [arXiv:0805.1451 [gr-qc]].
- [18] H. S. Reall, “Higher dimensional black holes and supersymmetry,” *Phys. Rev. D* **68** (2003) 024024. [hep-th/0211290].
- [19] S. S. Gubser and I. Mitra, “The evolution of unstable black holes in anti-de Sitter space,” *JHEP* **0108** (2001) 018 [arXiv:hep-th/0011127].
- [20] A. Buchel, “Bulk viscosity of gauge theory plasma at strong coupling,” *Phys. Lett. B* **663** (2008) 286-289. [arXiv:0708.3459 [hep-th]].
- [21] M. M. Caldarelli, R. Emparan and M. J. Rodríguez, “Black Rings in (Anti)-deSitter space,” *JHEP* **0811** (2008) 011 [arXiv:0806.1954 [hep-th]].
- [22] J. Armas and N. A. Obers, “Blackfolds in (Anti)-de Sitter Backgrounds,” *Phys. Rev. D* **83** (2011) 084039. [arXiv:1012.5081 [hep-th]].
- [23] J. Camps, R. Emparan, P. Figueras, S. Giusto, A. Saxena, “Black Rings in Taub-NUT and D0-D6 interactions,” *JHEP* **0902** (2009) 021. [arXiv:0811.2088 [hep-th]].
- [24] M. M. Caldarelli, R. Emparan, B. Van Pol, “Higher-dimensional Rotating Charged Black Holes,” *JHEP* **1104** (2011) 013. [arXiv:1012.4517 [hep-th]].
- [25] R. Emparan, T. Harmark, V. Niarchos and N. A. Obers, “Blackfolds in supergravity and string theory,” to appear.
- [26] G. Grignani, T. Harmark, A. Marini, N. A. Obers and M. Orselli, “Heating up the BIon,” [arXiv:1012.1494 [hep-th]].